



Analytical and computer modeling of thermal processes of laser interaction with single nanoparticle

Journal:	<i>RSC Advances</i>
Manuscript ID:	RA-ART-07-2014-007772.R1
Article Type:	Paper
Date Submitted by the Author:	19-Sep-2014
Complete List of Authors:	Smetannikov, Andrei; A.V.Luikov Heat and Mass Transfer Institute, Pustovalov, Victor; Belarusian National Technical University,

Cite this: DOI: 10.1039/c0xx00000x

www.rsc.org/xxxxxx

ARTICLE TYPE

Analytical and computer modelling of thermal processes of laser interaction with single nanoparticle

Victor K. Pustovalov^a and Andrei S. Smetannikov^b*Received (in XXX, XXX) XthXXXXXXXXXX 20XX, Accepted Xth XXXXXXXXXXXXX 20XX*

DOI: 10.1039/b000000x

The problem of optical (laser) radiation heating of nanoparticle (NP) is important for the applications in laser processing of NPs (laser induced transformation of NP size, shape and structure), light-to-thermal energy conversion and nanoenergy, laser nanomedicine, thermal catalysis, etc. It is essential to theoretically describe the temporal and spatial-temporal behavior of the NP and medium temperature for the analysis of experimental results and for theoretical prediction of the unknown dependences and new effects. Analytical and computer descriptions of heating, melting of single NP under action of CW and pulsed optical (laser) radiation and NP cooling after the termination of radiation action is carried out. Developed analytical model for the description of NP heating, heat dissipation and exchange with an ambience and its cooling has been examined and its accuracy and the applicability has been estimated and established.

Introduction

The advances in photo-thermal (PT) nanotechnology, that are based on the thermal effects and the processes induced by the laser–nanoparticle (NP) interaction, have been demonstrated their great potential.^{1–20} In the recent years absorption of radiation energy by NP, its heating, heat dissipation and exchange with an ambience, and following thermal and accompanied phenomena induced by laser–NP interaction have become an increasing important topics in nanotechnology.^{1–20} The problem of laser pulse heating of NP is important for various applications. Many reasons exist for this interest, including PT applications of NPs in different fields, such as laser processing of NPs (laser induced transformation of NP size, shape and structure),^{1–9} light-to-thermal energy conversion and nanoenergy,^{10–13} laser nanomedicine, photothermolysis of single cells and photothermally activated drug and gene delivery and release,^{14–18} thermal catalysis,^{19, 20} etc.

Most of these technologies rely on the position and the strength of the surface plasmon resonance on a nanosphere and absorption of radiation energy.^{21–25} During past years many research efforts have been focused on the investigation of unique size-dependent physical and chemical properties of the metallic NPs. The plasmonic properties of nanoscale metal NPs depend on different parameters, such as their dimensions, shapes, optical properties of metal and surrounding medium.^{22–25} Among others gold and silver NPs are known for their interesting optical properties and applications caused by the plasmonic resonances with significant absorption and scattering at the wavelengths of ~ 530 nm and ~ 400 nm respectively.^{1–25}

The prospects of NP applications in PT nanotechnology are strongly connected with modern achievements in laser physics,

nonlinear optics, chemistry, material sciences. The processes of chemical synthesis and the properties of homogeneous and two-layered NP have been presented.^{26–28} Different liquids (water, blood, bioliquids, etc.), dielectrics (silica, glasses, polymers, etc.) were used as ambient media under radiation-NP interaction.^{1–18} The pressure in medium, containing NPs, is frequently supposed constant during radiation-NP interaction.

It is important to theoretically describe the temporal and spatial-temporal behaviour of the NP and medium temperature for analysis of the experimental results and for the theoretical prediction of unknown dependences and new effects. Computer and analytical modeling are widely used for description of different processes and can be applied for these purposes. Analytical modeling has a few advantages in comparison with computer one because its results much simpler for the use and can be used for description of different experiments. On the other hand, the accuracy (precision) and the regions of applicability of analytical results should be estimated and established.

In this paper the developed analytical model of the description of NP heating, heat dissipation and exchange with an ambience will be examined and its accuracy and the applicability has been estimated and established. Analytical and computer descriptions of heating, melting of single NP under action of CW and pulsed optical (laser) radiation and its cooling after the termination of radiation action is carried out. The dependences of NP temperature on time during the processes of NP heating and cooling, heat exchange of heated NP with environment will be investigated. It is very important to take into account the temperature dependences of optical and thermo-physical parameters of NPs and surrounding media under the investigation of absorption of laser radiation, nanoparticle heating, heat transfer

and its cooling after the end of laser pulse action. The heat localization within the NP volume during some time interval without heat exchange with ambience (NP thermal confinement) will be investigated.

It is important to verify of proposed analytical model and its solutions and to determine the areas of their applications and accuracy on the base of comparison with numerical calculations, to review numerous theoretical articles investigating this problem, establish the important differences and new results in this article in comparison with other ones.

1. Analysis of theoretical models

A few theoretical models have been developed and applied for the description of the NP heating by laser radiation and the NP cooling and following processes.

The numerical modeling of the NP heating by laser radiation was carried out.^{17, 30-33} The short pulse laser interaction with a metal NP surrounded by water has been investigated,³⁰ based on the hydrodynamic computational model that includes a realistic equation of state for water and accounts for thermoelastic behaviour and the kinetics of electron-phonon equilibration in the NP. This radiation regime is suitable for targeted generation of thermal and mechanical damage of the sub-cellular level. The calculation on the base of hydrodynamic code with possible crack formation in silica embedded with NPs was carried out.³¹

The investigation³² is limited the case of intensive evaporation of NP material and in contradiction with³⁰ the investigation of the processes in the environment did not carry out. The two-temperature model for electron and lattice systems inside NP was taken into account together with heat exchange with ambience.³⁰

The processes in electron-lattice system have been finished by instant $t \leq 10^{-12}$ s without significant heat exchange with ambience and hydrodynamic processes.^{34, 35} The heat conduction from NP and other thermal processes is commenced for $t > 10^{-12}$ s. The investigation of these processes can be divided in time and conducted separately. Inclusion of two-temperature model in description of thermal and hydrodynamic processes inside and around NP looks like as unnecessary.

The process of heating of a spherical gold NP by nanosecond pulses and the heat transfer between the NP and the surrounding medium with no mass transfer have been numerically modeled by finite element method.³³ The thermal conductivity changes, vapor formation, and changes of the dielectric properties were included in this investigation.

Analytical modeling of the NP heating by laser radiation was carried out.³⁵⁻⁴⁰ The analytical solutions are much simpler and useful for description of thermal processes than computer results, but without high accuracy. The approaches are based on steady-state situation using only energy conservation equation, when the equality exists between heat input to NP by the transduction of resonant irradiation (absorbing energy by NP) and outward heat flux by the conduction at thermal equilibrium.³⁸⁻⁴⁰ The energy balance was applied to obtain a macroscale heat-transfer time constant. This approach works only for CW irradiation and radiation pulses with long pulse durations.

The estimation of characteristic time τ_0 for the cooling of a spherical particle was used in on the assumption of equating of heat capacity of the NP to the heat capacity of a layer of the

surrounding fluid with the thickness of the thermal diffusion length.³⁸ No basis or confirmation of this assumption has been presented. Interface thermal conductance is treated as an adjustable parameter that can be determined from experiments.³⁸

Two problems are worth discussing in laser heating of NP and its cooling that. A first problem is the applicability of the diffusive heat equation to nanoscale thermal processes that requires justification. It was noted, that the diffusive equation is valid if the mean free path of the heat carriers—electrons, phonons in NP and molecules, phonons, etc. in ambient medium is smaller than the characteristic NP size.⁴⁰ In amorphous surrounding solids and liquids, the mean free path is very short $\sim 10^{-8}$ cm and it is of the order of atomic distances. The length of free path of water molecule in ambient water is about of ~ 0.1 nm and this one is much smaller than characteristic NP radii of $r_0 \sim 10-100$ nm. Consequently, the heat flow in liquids, amorphous solids can be well described by the diffusive heat equation, when nanoscopic length scales are involved.

The mean free path of molecules is about $\sim 5 \cdot 10^{-6}$ cm in gases at atmospheric pressure and diffusive heat equation can be applied for heat exchange of NP with surrounding gaseous medium for $r_0 \geq 100$ nm. In this case, the methods of kinetic equation or molecular dynamics should be used. For gas pressure ~ 100 atm and more and normal temperature ~ 300 K diffusive heat equation can be used for $r_0 \geq 10$ nm. We do not investigate the gases as ambient media because this topic is out of our interest.

A second problem is the presence of possible surface thermal resistivity at the surface of NP immersed in a liquid or solid ambience. A thermal resistivity may occur because of the material discontinuity, surface nanoscale roughness, etc. and can play important role in some cases, such as hydrophobic coating of NP surface by some liquids, or bad contact of solid ambient material with NP surface.¹³ The nature and the regions of existence of interface thermal resistivity (conductance) should be cleared and confirmed by the experiments or complicated computer modeling of the processes on NP surface in different ambiances. But in many situations NP surface resistivity does not have any significant effect and we use the condition of “ideal” heat contact between NP surface and ambient medium.

The analytical solutions of heat transfer equation were applied in the region outside the NP sphere for some special conditions, e.g. a constant heat flux boundary condition at the NP surface.⁴⁹ But these solutions can not be used for description of real processes of NP laser heating.

Unfortunately there is no self-consistent analytical theory³⁸⁻⁴⁰ including only real parameters of NP material, environment and laser radiation how it follows from previous analysis. Theory has to be self-consistent without using of empirical or adjustable (fitting) parameters that were determined from experiments or used for achievement of some agreement of theoretical dependences with experimental once.

The analytical model^{35,36} demonstrates some advantages in comparison with previous analytical approaches. The temperature dependences of optical and thermo-physical parameters of NPs and surrounding media were taken into account under investigation of absorption of laser radiation, electron-phonon coupling, NP heating, heat transfer and its cooling after the end of laser pulse action.^{35,36} Theoretical modeling of the processes of

laser-NP interaction and analytical nonlinear solutions for quasi-steady distributions of temperature T and heat flux on radius r around spherical NP and temporal dependences of NP temperature T_0 on t have been carried out and investigated. But the basement and determination of the application regions and accuracy of this model have not been carried out.

Verification of accuracy and regions of applicability of analytical model^{35,36} is carried out in this article. The processes of radiation-NP interaction will be considered under condition of the equality of electron and lattice temperatures for the pulse durations $t_p \geq 1 \cdot 10^{-12}$ s.

2. Computer and analytical models

Parameters of nanoparticles and radiation

Different parameters of the optical (laser) radiation, spherical NP and the ambient medium can influence on the thermo-optical properties of absorbing NPs and determine the achievement of the maximal efficiency of absorbed energy conversion into PT phenomena. We note the following set of parameters:

radiation – a) pulse duration t_p , b) wavelength λ , c) energy exposure (density) E_0 (intensity I_0);

nanoparticle – a) the material of homogeneous NP with own values of density ρ_0 , heat capacity c_0 , thermal conductivity k_0 , optical indexes, etc., b) optical properties, c) size, d) shape (spherical).

ambient medium – a) coefficient of thermal conductivity k_m , density ρ_m , heat capacity c_m , b) coefficient of absorption, scattering and extinction.

The investigation of the optical properties of NPs, when placed in media, is a prerequisite for the successful thermal applications of NPs and had been conducted.²²⁻²⁶ The optical properties (efficiency factors of absorption K_{abs} , scattering K_{sca} and extinction K_{ext}) for metallic spherical NPs with the radii $r_0 = 10, 25, 50$ nm, placed in water, for radiation with wavelengths in the range 250-1100 nm are presented.²⁶

It is important to consider NP sizes within the range of ~ 10 -100 nm realizing most interesting and useful effects and phenomena in nanooptics, laser (optical) and nanomedicine applications. For nanomedicine applications (cancer treatment) NPs smaller than 10 nm are rapidly eliminated through the kidney and NPs within 10-100 nm travel throughout the blood stream and can leak into the tumor tissue owing to the abnormal tumor blood vessels.¹⁴⁻¹⁸ The dependences of NP properties on their sizes cannot be taken into account for the values of NP radii in the range $10 < r_0 < 100$ nm.

Computer model

The thermal processes of radiation-NP interaction include the absorption of radiation energy by NP and its heating, heat transfer into ambience and NP cooling after the termination of action. The heat conduction equation for spherical geometry:¹⁷

$$c_i \rho_i \frac{\partial T}{\partial t} = \frac{1}{r^2} \frac{\partial}{\partial r} \left(r^2 k_i \frac{\partial T}{\partial r} \right) + q_i \quad (1)$$

T is the temperature, r is the radius of the spherical coordinate system with the origin fixed at NP centre, t is time, c_i , ρ_i , k_i are

heat capacity, density and thermal conductivity respectively, the NP parameters are determined for $r \leq r_0$ ($i = 0$) and the ambient medium parameters are determined for $r > r_0$ ($i = m$), q_i is the power density of heat sources ($r \leq r_0$ $q_0 = I_0 K_{abs} \pi r_0^2 / V_0$, I_0 – intensity of radiation, K_{abs} – absorption efficiency factor of radiation with wavelength λ by NP with radius r_0 , $q_m = 0$ for $r > r_0$), $V_0 = 4/3 \pi r_0^3$ is the volume of NP, with the initial condition:

$$T(r, t = 0) = T_\infty \quad (2)$$

T_∞ – the initial temperature of NP and medium. The differential equation (1) is approximated with implicit finite-difference scheme second order of accuracy in time and space (Crank-Nikolson scheme). For numerical solution of finite-difference equation a sweep method is used.

Analytical model

Analytical model of the thermal processes of radiation-NP interaction is based on two main assumptions – a first one is the use of uniform temperature inside NP volume during heating and cooling of NP, a second one is the use of the quasi-stationary heat exchange of NP with ambience (quasi-stationary dependence of T on r for $r > r_0$), that allow to get analytical solutions. The equation with uniform temperature T_0 over the particle volume, that describes the heating and cooling of a NP, has the form:^{35, 36}

$$\rho_0 c_0 V_0 \frac{dT_0}{dt} = \frac{1}{4} I_0 K_{abs} S_0 - J_C S_0, \quad (3)$$

with initial condition:

$$T_0(t = 0) = T_\infty. \quad (4)$$

$$\int_0^{r_0} q_0 4\pi r^2 dr = \frac{1}{4} I_0 K_{abs} S_0,$$

$S_0 = 4\pi r_0^2$ is the surface area of spherical NP of radius r_0 , ρ_0, c_0 – density and heat capacity of NP material respectively, J_C is the energy flux density from NP by mechanism of heat conduction. Convective and hydrodynamic heat transfer from NP is negligible for variants in our considerations. The radiation cooling of NP is equal $J_R \approx \sigma(T_0^4 - T_\infty^4) \ll J_C$ for $T_0 < 5 \cdot 10^3$ K, σ – Stefan-Boltzmann constant.⁴⁴ The energy losses J_C at NP surface due to heat conduction is equal

$$J_C = -k_m(T) \frac{dT}{dr} \quad (5)$$

k_m – thermal conductivity coefficient of a surrounding medium. Ideal thermal contact is assumed between NP surface and ambient medium.

The heating of NP up to high temperatures leads to necessity taking into account the dependences of optical and thermal properties of NPs and ambient media on temperature. The dependence of the coefficient of thermal conductivity of the surrounding medium k_m on temperature T can be presented in next forms:

$$k_m = k_\infty (T/T_\infty)^a \quad (\text{a}), \quad k_m = k_\infty \exp[\varepsilon(T - T_\infty)] \quad (\text{b}) \quad (6)$$

$k_\infty = k_m(T=T_\infty)$, parameters $a = \text{const}$, $\varepsilon = \text{const}$ (for example, for water under saturation pressure $a \approx 0.5$ in the temperature range $273 < T < 473$ K⁴⁴).

The characteristic time for the formation of quasi-stationary distribution of temperature in ambient medium for spherical geometry is equal:

$$t_T = \frac{c_m \rho_m r_0^2}{4k_m} \quad (7)$$

for $r_0 = 25$ nm and $k_m = 6 \cdot 10^{-3}$ W/(cm K) (water)⁴⁶ $t_T \sim 10^{-9}$ s. If the pulse duration t_p is bigger than t_T , the approximation of the quasi-stationary (steady) temperature distribution and heat exchange between a NP and its environment can be applied. The quasi-stationary temperature distribution for $r \geq r_0$ around a NP and heat flux J_C from NP at $r=r_0$ under condition $t > t_T$ was obtained from (1) under $\partial T / \partial t = 0$ taking into account (6a):^{35,36}

$$r \geq r_0, \quad a \neq -1, \quad T(r) = T_\infty \left[1 + \frac{r_0}{r} \left(\left(\frac{T_0}{T_\infty} \right)^{a+1} - 1 \right) \right]^{\frac{1}{a+1}}, \quad (8)$$

$$J_C = \frac{k_\infty T_\infty}{(a+1) r_0} \left[\left(\frac{T_0}{T_\infty} \right)^{a+1} - 1 \right].$$

These solutions are taking into account the temporal dependences $T_0(t)$ during NP heating and cooling and this approximation consists in the using of quasi-stationary solution (8) for the transient problem (equation (3)). The solutions for the case $a = -1$ are presented.^{17, 36}

The dependences of K_{abs} on the temperature T_0 for NPs from different materials can be presented in the forms:

$$K_{abs} = K_\infty (T_0 / T_\infty)^b \quad (\text{a}),$$

$$K_{abs} = K_\infty \exp[\varepsilon_0 (T_0 - T_\infty)] \quad (\text{b}) \quad (9)$$

$K_\infty = K_{abs}(T_0 = T_\infty)$, parameters $b = \text{const}$, $\varepsilon_0 = \text{const}$. Dependence of $K_{abs}(T_0)$ is presented, for example, for Al_2O_3 NP.³⁵

For constant $K_{abs} = K_\infty \approx \text{const}$, $b=0$ (9a) and temperature dependence $k = k_\infty (T/T_\infty)^a$ (6a) we have analytical solutions for temporal dependence $T_0(t)$ from (3, 4, 5, 8) for the period of time $0 \leq t \leq t_p$:

$$a = 0, \quad T_0 = T_\infty + \frac{I_0 K_{abs} r_0}{4k_\infty} [1 - \exp(-t / \tau_0)] \quad (10)$$

$$a = 1, \quad T_0 = T_\infty A \frac{A + 1 - (A - 1) \exp(-t / \tau_1)}{A + 1 + (A - 1) \exp(-t / \tau_1)} \quad (11)$$

$$\tau_0 = \frac{c_0 \rho_0 r_0^2}{3k_\infty}, \quad A = \left(\frac{I_0 K_{abs} r_0}{2k_\infty T_\infty} + 1 \right)^{1/2}$$

$$\tau_1 = \tau_0 \frac{(2T_\infty k_\infty)^{1/2}}{(I_0 K_{abs} r_0 + 2k_\infty T_\infty)^{1/2}}. \quad (12)$$

We note that characteristic time τ_0 describing the processes of NP

heating and cooling was mistakenly used in¹³ for the description of steady-state temperature profile. The cooling of NP can be described by expression, which can be derived from (3) with use (6, 8) under $I_0 = 0$, $T(t=t_p) = T_{max}$ and $t > t_p$:

$$a = 0, \quad T_0 = T_\infty + (T_{max} - T_\infty) \exp(-(t - t_p) / \tau_0) \quad (13)$$

$$a = 1, \quad T_0 = T_\infty \frac{B + 1 + (B - 1) \exp(-(t - t_p) / \tau_1)}{B + 1 - (B - 1) \exp(-(t - t_p) / \tau_1)},$$

$B = T_{max}/T_\infty$, T_{max} is the maximal value of the temperature at the end of laser pulse $t=t_p$ in (10, 11). The analytical solutions for the use of different combinations of temperature dependences of $K_{abs}(T_0)$ and $k_m(T)$ have been presented.³⁴

3. Computer and analytical modeling of nanoparticle heating by radiation and discussions

Fig. 1,2 (left column) presents the temporal-spatial distributions of the temperature $T(r)$ inside and around NP for the different time instants for spherical gold NP with $r_0 = 25$ nm, placed in water, for CW and pulsed irradiation with the pulse durations $t_p = 10^{-2}$, 10^{-4} , 10^{-6} , 10^{-8} , 10^{-10} s, 10^{-12} s, values of normalized radiation intensity $I_n = I_0 K_{abs}$, based on the computer calculations of the equations (1,2). Maximal values of $T(r=r_0)$ for all variants are smaller than boiling temperature of water $T_b = 373$ K⁴⁴ (see Figs. 1, 2) at outer atmospheric pressure $p=1$ atm and we avoid the necessity to take into account the formation of vapor bubble around heated NP. CW and pulsed radiation causes an intensive heating of NP during its action.

It can be noted that the temperature profile, which takes a certain form after the lapse of some interval of time from the irradiation start, rises without changing it with time up to termination of pulse. The temperature inside NP is being virtually independent of the coordinate r , $T(r) \approx \text{const}$, $r \leq r_0$, for different instants of time and values of radiation intensity. This weak temperature gradient inside NP exists for all values of t_p during radiation action from CW to $t_p = 1 \cdot 10^{-12}$ s (since thermal diffusivity of metals considerably higher than surrounding medium).

Temperature drop is being observed in the adjacent layer of the surrounding medium. The specific feature for CW and pulsed irradiation for the range of pulse durations of $t_p = 10^{-2}$ - 10^{-8} s is the presence of developed NP heat transfer with the surrounding medium during the radiation action. Temperature distributions on r outside of NP for lines 1-3 (1-5) in Fig. 1 practically coincides each other for a few time instants. It means the formation of stationary temperature profiles for CW and pulsed irradiation with $t_p \sim 10^{-2}$ - 10^{-6} s (see Fig. 1). On the other hand, a non-stationary character of NP heat exchange with the surrounding medium (water) is confirmed by the computer simulation for short laser pulses $t_p \sim 10^{-8}$ - 10^{-12} s. It means practically absent or weak heat exchange of NP with the surrounding and heat localization of absorbed laser pulse energy in NP leading to its considerable heating in excess of the surrounding medium.

The computer distributions show main feature - approximate

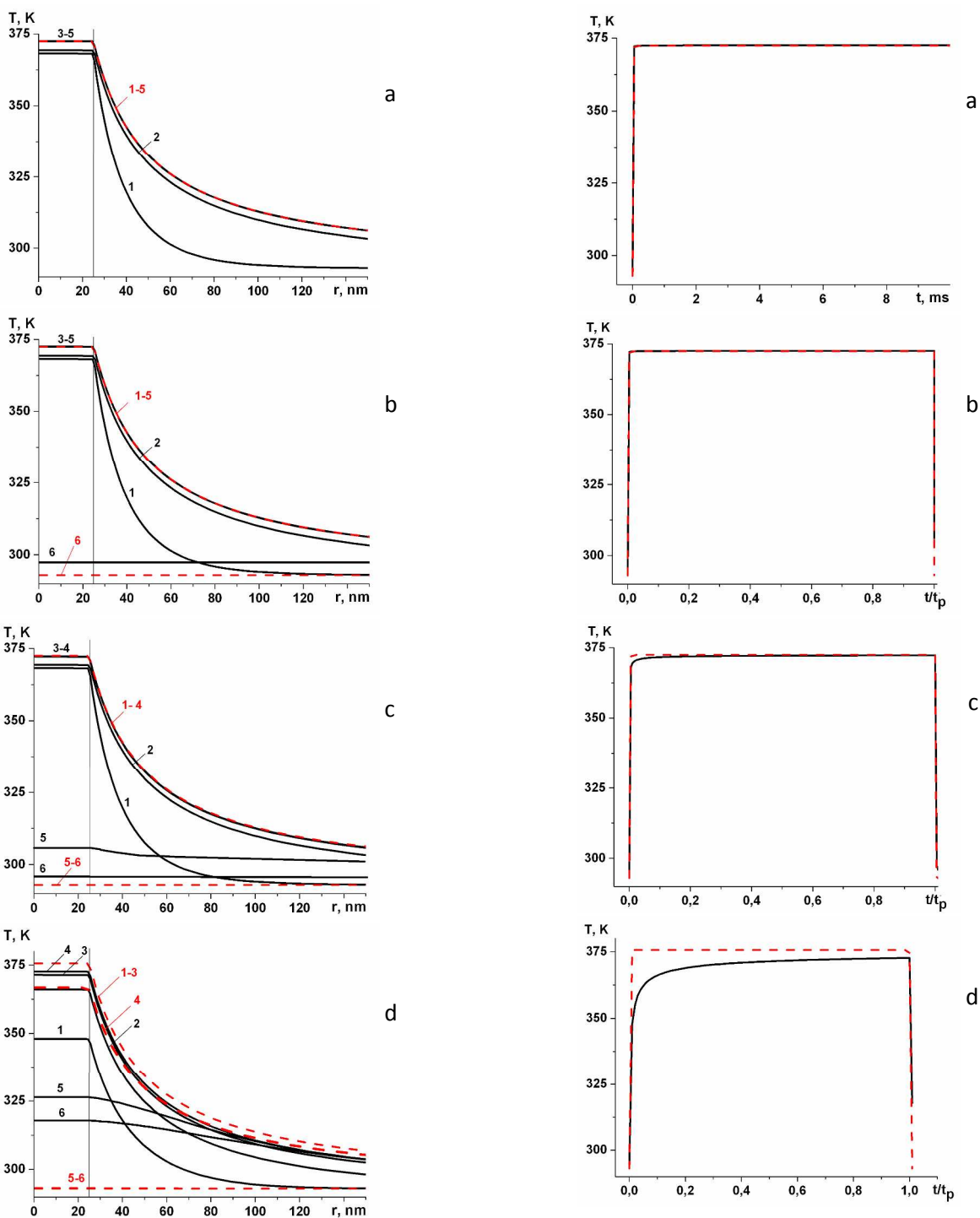


Fig. 1 Computer (solid) and analytical (dashed) dependences of the temperature T along the radius r for the time instants t/t_p (left column) and temporal dependences of T_{max} ($r=0$) (right column) for Au NP with $r_0=25$ nm, placed in water: for CW irradiation on $t - I_n = 0.75$ MW/cm², $t = 1 \cdot 10^{-8}$ (1), $1 \cdot 10^{-6}$ (2), $1 \cdot 10^{-3}$ (3), $5 \cdot 10^{-3}$ (4), $1 \cdot 10^{-2}$ s (5) (a); for pulsed irradiation on $t/t_p - t_p = 1 \cdot 10^{-2}$ s, $I_n = 0.75$ MW/cm², $t/t_p = 1 \cdot 10^{-6}$ (1), $1 \cdot 10^{-4}$ (2), 0.1 (3), 0.5 (4), 1 (5), 1.00001 (6) (b); $t_p = 1 \cdot 10^{-4}$ s, $I_n = 0.75$ MW/cm², $t/t_p = 1 \cdot 10^{-4}$ (1), $1 \cdot 10^{-2}$ s (2) 0.5 (3), 1.005 (5), 1.01 (6) (c); $t_p = 1 \cdot 10^{-6}$ s, $I_n = 0.78$ MW/cm², $t/t_p = 1 \cdot 10^{-2}$ (1), 0.1 (2), 0.5 (3), 1.0 (4), 1.005 (5) 1.01 (6) (d). Vertical lines in left column present the boundary of NP.

uniform temperature over NP volume inside depending on t during radiation action and cooling for wide interval values of t_p (see Fig. 1, left column). The computer and analytical distributions of T along radius ($r > r_0$) practically coincide each other for CW and for the range of pulse durations $t_p = 10^{-2} - 10^{-6}$ s (Fig. 1 a-d), see indicators 1-5 denoted analytical and computer distributions. The quasi-stationary character of temperature distributions for $r > r_0$ and heat transfer from NP for $t_p > 10^{-7}$ s has been confirmed by computer results. These two features were applied for the construction of presented analytical model. For $t_p = 10^{-8}, 10^{-10}$ s the analytical distributions differ from

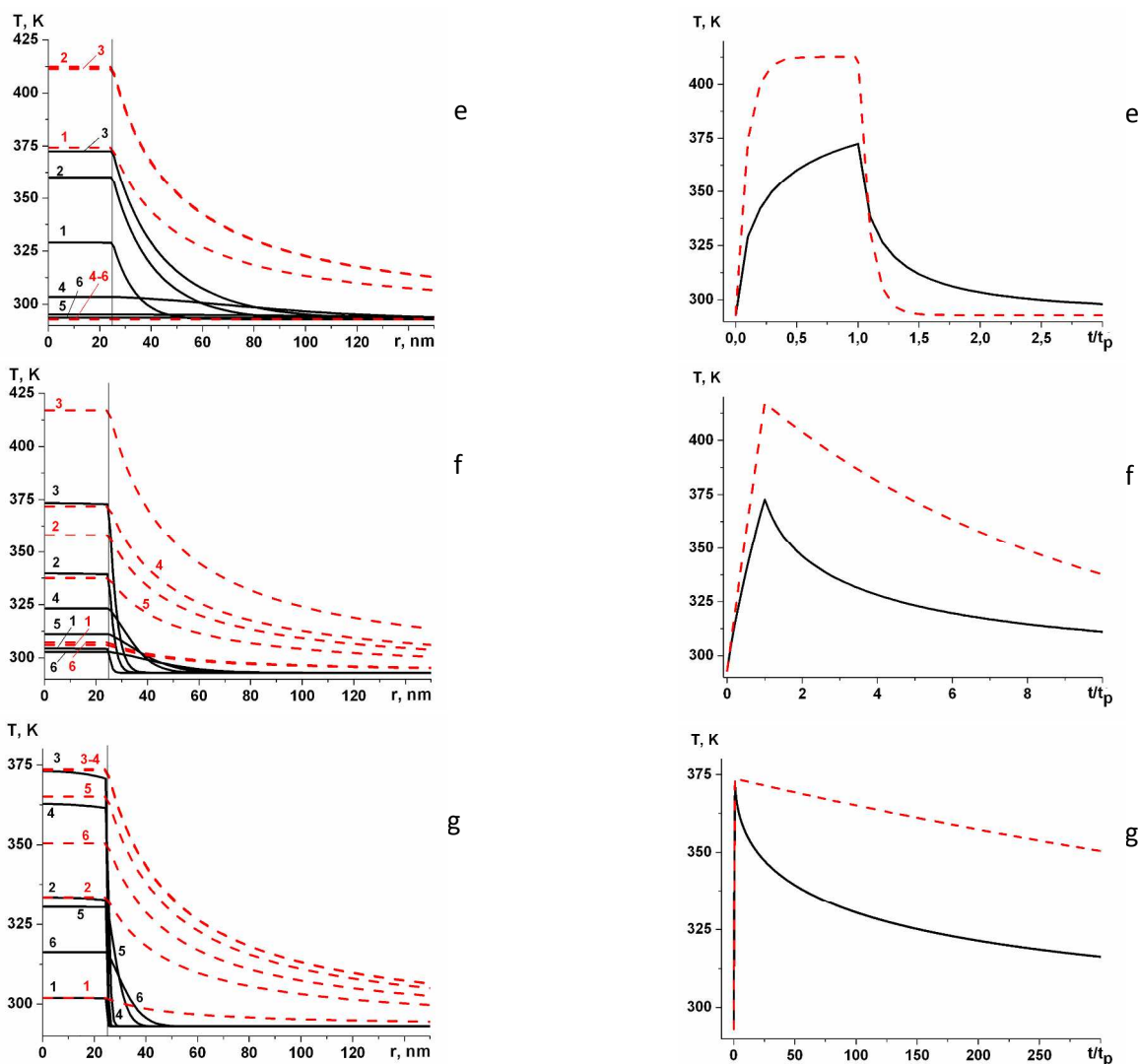


Fig. 2. Computer (solid) and analytical (dashed) dependences of the temperature T along the radius r for the time instants t/t_p (left column) and temporal dependences of $T_{max}(r=0)$ on t/t_p (right column) for pulsed irradiation - for $t_p=1\cdot 10^{-8}$ s, $I_0=1.13$ MW/cm², $t/t_p=0.1$ (1), 0.5 (2), 1.0 (3), 2.0 (4), 5.0 (5), 10.0 (6) (e); $t_p=1\cdot 10^{-10}$ s, $I_0=10.9$ MW/cm², $t/t_p=0.1$ (1), 0.5 (2), 1.0 (3), 5.0 (4), 10.0 (5) 20.0 (6) (f); for $t_p=1\cdot 10^{-12}$ s, $I_0=0.67$ GW/cm², $t/t_p=0.1$ (1), 0.5 (2), 1.0 (3), 5.0 (4), 100.0 (5) 300.0 (6) (g). Vertical lines in left column present the boundaries of NP.

computer ones up to 10-25 % inside and outside of NP volume and this behaviour is explained by non-stationary character of computer distributions of $T(r)$ for $r > r_0$.

For $t_p = 10^{-12}$ s the internal computer and analytical distributions of $T(r)$ during pulse duration are close to each other, because the heat exchange with ambience is practically absent in this case and temperature is determined of heat source (absorption energy).

computer ones up to 10-25 % inside and outside of NP volume and this behaviour is explained by non-stationary character of computer distributions of $T(r)$ for $r > r_0$.

For $t_p = 10^{-12}$ s the internal computer and analytical distributions of $T(r)$ during pulse duration are close to each other, because the heat exchange with ambience is practically absent in this case and temperature is determined of heat source (absorption energy).

But temperature distributions outside of NP for $r \geq r_0$ differ significantly because of non-stationary character for computer

25

distributions of $T(r)$ and quasi-stationary character of analytical dependences $T(r)$.

Figures 1, 2 (right column) show the temporal dependences of the maximal temperature at the centre of gold NP $T_{max}(r=0, t)$ on t/t_p for different pulse durations and on t for CW irradiation determined on the base of the computer calculations of (1,2) and the analytical dependences (10-13). Immediately after irradiation commencement for CW and for $t_p = 10^{-2} - 10^{-12}$ s the heating of the NP and its heat exchange with the surrounding water start.

30

The temporal dependences of $T_{max}(r=0)$ on t have the significant features for different values of t_p .

For CW and $t_p = 10^{-2} - 10^{-4}$ s the heating of NP up to maximal temperature T_{max} is realized very rapidly after that the absorption of energy is compensated by heat losses because of the heat conduction. The temperature $T(r=0)$ achieves the value of $\sim T_{max}(r=0)$ to the time instant $t \sim (0.01-0.1)t_p$.

40

For $t_p = 10^{-6}$ s the temperature $T(r=0)$ achieves the value of $0.9T_{max}(r=0)$ up to time instant $t = 0.1t_p$ and during the rest part of t_p slowly achieved $T_{max}(r=0)$. After the laser pulse with $t_p = 10^{-2} - 10^{-6}$ s is turned off, a NP gives up energy to medium for time interval about 10^{-8} s, and its temperature T_0 moves down and becomes equal initial temperature T_0 . For $t_p \leq 10^{-6} - 10^{-8}$ s the

45

temperature $T(r=0)$ achieves the value of $T_{max}(r=0)$ to the end of pulse action.

NP is heating by shorter laser pulses with $t_p = 10^{-8}$ – 10^{-12} s during pulse action up to $T_{max}(r=0)$ and the cooling is carried out with the characteristic times 10^{-10} – $10^{-3} t_p$ (see Fig. 2). The excess heating of the NP with respect to medium generally depends on the local value of the intensity, size and optical characteristics of the NP among other parameters.

For ultrashort pulse with $t_p = 10^{-12}$ s the analytical dependence $T_\theta(t)$ (dashed lines) describing of temporal cooling of NP slowly decreases in comparison with the computer dependence, because non-stationary temperature gradient is more sharp than the analytical quasi-stationary gradient. For intermediate case with pulse duration $t_p = 10^{-8}$, 10^{-10} s analytical value of T_{max} is bigger than the computer value of T_{max} , because non-stationary heat exchange of NP takes place during laser pulse action. Analytical expressions describe temporal behavior of NP temperature during its heating by laser pulse and cooling with sufficient accuracy for the ranges $10^{-12} \leq t_p \leq 10^{-11}$ s and the heating and cooling in the interval of time $10^{-11} < t_p < 10^{-8}$ s with errors ~ 20 – 30% .

These comparisons and definite coincidences of analytical results with computer results of heating of NPs by short laser pulses validate developed analytical model. Computer simulation confirms the possibility to use analytical model for the description of the temporal dependence of NP temperature T_θ with sufficient accuracy for CW irradiation and for the range $t_p > 10^{-7}$ s for NP heating and cooling processes, for NP heating for time interval $10^{-12} \leq t_p \leq 10^{-11}$ s, and for the description of the outward distributions $T(r)$ for $t_p \geq 10^{-7}$ s and for CW irradiation.

30 Thermal confinement

The characteristic times τ_θ and τ_l determine the temporal dependences of T_θ (13, 14). The pulse duration t_p should be less than the characteristic times τ_θ (τ_l) of NP cooling to provide efficient heating of NPs without heat loss [1, 13]. The fulfilment of thermal confinement means achievement of maximal value of NP temperature $T_{max} = T_\theta(t_p)$ and saving own heat energy practically without heat exchange with ambience during “short” pulse action with $t_p < \tau_\theta$. In this case we find from (13) the following equation for $0 < t \leq t_p$:

$$40 \quad t_p < \tau_\theta, T_\theta \approx T_\infty + \frac{3I_0 K_{abs} t}{4\rho_0 c_0 r_0}, \quad (14)$$

In the opposite case (“long” radiation pulses) the condition of NP thermal confinement is interrupted for $t_p > \tau_\theta$ and heat loss from NP by heat conduction have to be taken into account during the period of time $0 \leq t \leq t_p$. The case $t_p > \tau_\theta$ can be used for intensive heat exchange of NPs with an ambience and its heating. In this case from (13) we have

$$t_p < \tau_\theta, T_\theta \approx T_\infty + \frac{I_0 K_{abs} r_0}{4k_\infty} \quad (15)$$

For CW irradiation we have from (13) for $a=0$ the equation (15) and for $a=1$:

$$50 \quad T_\theta \approx T_\infty \left(\frac{I_0 K_{abs} r_0}{2k_\infty T_\infty} + 1 \right)^{1/2}.$$

Figure 3 presents the dependences of characteristic times of formation of quasi-steady spatial distribution of temperature around NP $t_T = c_m \rho_m r_0^2 / (4k_m)$ (7) and of NP cooling $\tau_0 = c_0 \rho_0 r_0^2 / (3k_m)$ (12) for $a=0$. These characteristic times have quadratic dependences on r_0 , but t_T (7) depends on different thermal constants of medium and τ_0 (12) depends on NP and medium parameters.

The dependences of τ_{T0} and t_T on r_0 for gold NPs placed in surrounding water and silica are presented in Fig. 3. It is interesting to note that $\rho_\theta c_0 = 2.49$ for gold and 2.48 for silver and Fig. 3 can be approximately used for both metallic NPs simultaneously. The characteristic time τ_T is equal $\tau_T \sim 3 \cdot 10^{-11}$ – $1.2 \cdot 10^{-8}$ s for the range $r_0 = 5$ – 100 nm and for ambient water with $k_m = 6 \cdot 10^{-3}$ W/(cm·K), $\tau_T \sim 0.9$ ns for $r_0 = 25$ nm (Fig. 1). The fulfilment of the condition $t_p < \tau_T$ for most interesting range of r_0 : $r_0 \leq 50$ nm means that the value of t_p will be in the range of pulse durations: $t_p \leq 3 \cdot 10^{-9}$ s.

Energetic parameters

Of interest is the study of the integral energy parameters that characterize the interaction of laser radiation with a NP - its heating, melting, cooling from the onset of irradiation $t = 0$ to the time considered t : the quantity of radiation energy Q_{abs} absorbed by a NP, the quantities of heat spent for NP melting Q_M and removed from a NP by heat conduction Q_C , and also the thermal energy of a NP E_T :

$$Q_{abs} = \pi r_0^2 \int_0^t I_0(t) K_{abs} dt, Q_C = 4\pi r_0^2 \int_0^t J_C dt, \quad (16)$$

$$E_T = \rho_0 c_0 V_0 T_0, Q_M = \rho_0 V_0 L_M,$$

for $I_0 = \text{const}$, $K_{abs} = \text{const}$, $Q_{abs} = \pi r_0^2 I_0 K_{abs} t$ for $t \leq t_p$, where L_M – heat of unit mass melting. Integration over the time $t = 0$ to t with regard for equation (4) and the energies (16) will give the energy conservation law for a NP:

$$Q_{abs} + E_{T_\infty} = E_T + Q_C + Q_M \quad (17)$$

$E_{T_\infty} = \rho_0 c_0 V_0 T_\infty$ is the initial thermal energy of a NP, energy $Q_M = 0$ under $T_0 < T_m$. Equation (17) can be used for the control of the energy conservation law of the processes of laser action on NP.

The energy Q_C can be analytically calculated using equation (16) and expressions for J_C (8), T (10) taking into account $T_{max} = T(t=t_p)$, $t_{max} = t_p$ under $a = 0$ for the period of time $[0, t_p]$:

$$Q_C(t) = Q_{abs}(t) \left[1 + \frac{\tau_0}{t} \left(\exp\left(-\frac{t}{\tau_0}\right) - 1 \right) \right] \quad (18)$$

90 and for $t > t_p$

$$Q_C(t) = Q_{abs}(t_p) \left[1 + \frac{\tau_0}{t_p} \exp\left(-\frac{t}{\tau_0}\right) \left(1 - \exp\left(\frac{t_p}{\tau_0}\right) \right) \right]. \quad (19)$$

The correlation between heat energy contained in NP and transferred in environment at current moment and in the course of time is very essential for initiation and realization different physical-chemical processes inside a NP and in surrounding.

We used next parameters for the estimations of the influence of different mechanisms of thermal processes and

$$P_1 = \frac{Q_{abs}}{Q_{sca}}, P_2 = \frac{Q_C}{Q_{abs}}, P_3 = \frac{Q_{abs} - Q_C}{Q_{abs}}. \quad (20)$$

The parameter P_1 describes the correlation between absorption

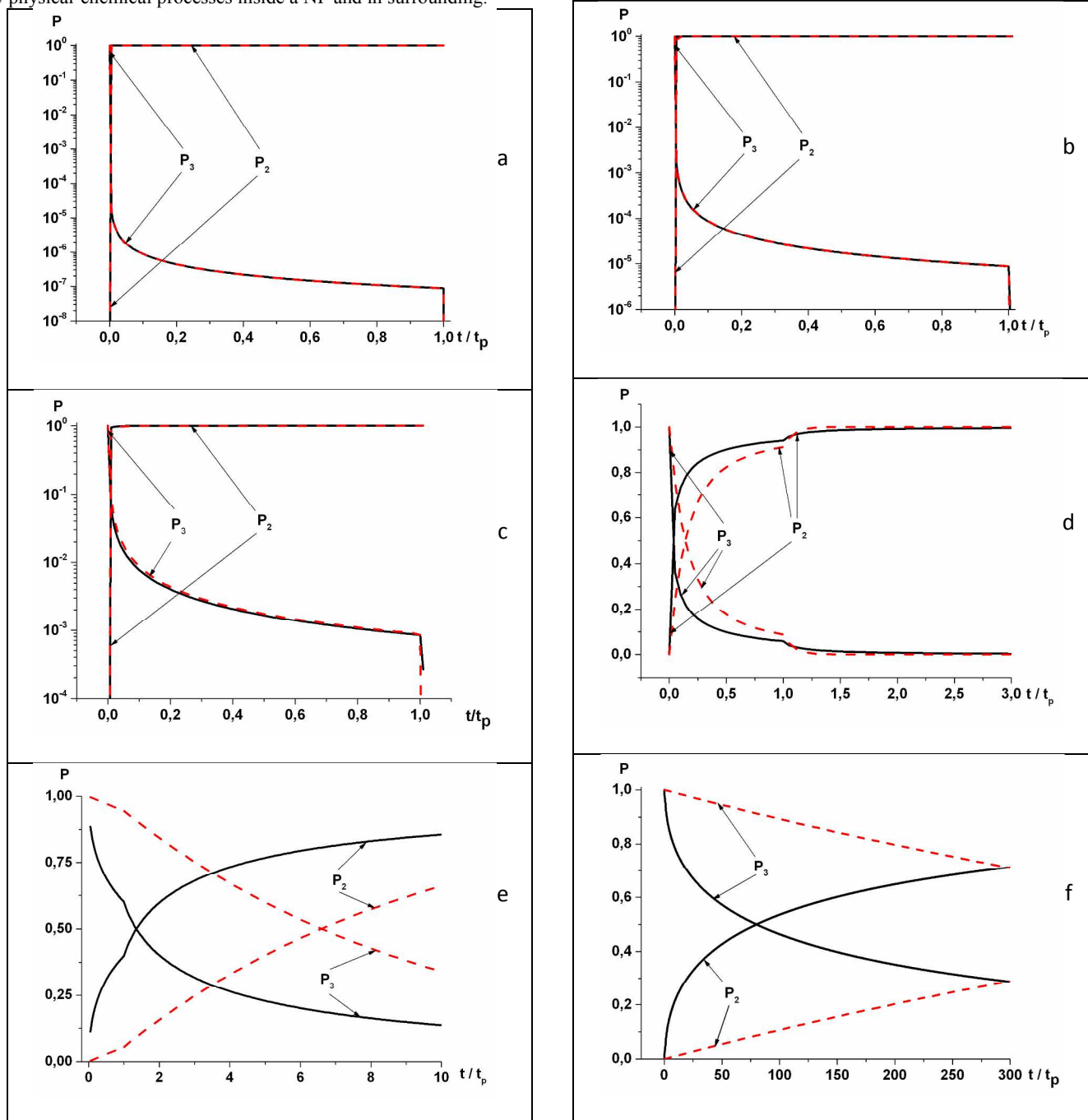


Fig. 3. Computer (solid) and analytical (dashed) dependences of the parameters of P_2 and P_3 on t/t_p for Au NPs with the radius $r_0 = 25$ nm for $t_p = 1 \cdot 10^{-2}$ s, $I_n = 0.75$ MW/cm² (a), $t_p = 1 \cdot 10^{-4}$ s, $I_n = 0.75$ MW/cm² (b), $t_p = 1 \cdot 10^{-6}$ s, $I_n = 0.78$ MW/cm² (c), $t_p = 1 \cdot 10^{-8}$ s, $I_n = 1.13$ MW/cm² (d), $t_p = 1 \cdot 10^{-10}$ s, $I_n = 10.9$ MW/cm² (e), $t_p = 1 \cdot 10^{-12}$ s, $I_n = 0.67$ GW/cm² (f).

and scattering of radiation by NP. The parameter P_1 is determined by optical characteristics of a NP and had been investigated for the metallic NPs.⁴⁵ The parameter of P_2 determines the correlation between heat loss energy by NP and absorbed energy by NP and P_3 determines the correlation between NP thermal

energy and absorbed energy during the heat exchange with ambience.

Parameters of P_2 and P_3 are determined by analytical expressions for $Q_C(t)$ (18, 19) and have the forms (21) for $0 < t \leq t_P$ and (22) for $t > t_P$:

$$P_2 = 1 + \frac{\tau_0}{t} \left(\exp\left(-\frac{t}{\tau_0}\right) - 1 \right), P_3 = \frac{\tau_0}{t} \left(1 - \exp\left(-\frac{t}{\tau_0}\right) \right), \quad (21)$$

$$P_2 = 1 + \frac{\tau_0}{t_P} \exp\left(-\frac{t}{\tau_0}\right) \left(1 - \exp\left(\frac{t_P}{\tau_0}\right) \right), \quad (22)$$

$$P_3 = \frac{\tau_0}{t_P} \exp\left(-\frac{t}{\tau_0}\right) \left(\exp\left(\frac{t_P}{\tau_0}\right) - 1 \right).$$

Computer (solid) and analytical (dashed) dependencies of the parameters P_2 , P_3 on t/t_P for Au NPs with the radius $r_0=25$ nm placed in water, were presented in Figure 3. Computer and analytical dependencies almost completely coincide with each other for $t_P = 10^{-2}-10^{-8}$ s. It means that analytical equations (21, 22) describe the computer dependencies with appropriate accuracy. It is interesting to note that for $t_P = 10^{-8}$ s computer and analytical dependencies of $T(r)$ for different time instants differ significantly (see Fig 1d). But the dependences of P_2, P_3 on t are approximately close each other. It could be explained by qualitative neighbouring of the dependencies of $T(r)$ for $t_P=10^{-8}$ s with quantitative difference in the values of $T(r)$ for computer and analytical results.

Figure 4 presents the analytical dependences of characteristic times of NP cooling $\tau_0 = c_0 \rho_0 r_0^2 / (3k_m)$ (12) for $a=0$ gold NP with $r_0=25$ nm, placed in water and in silica. These characteristic times have quadratic dependences on r_0 . Note, that τ_0 (12) depends on NP and medium parameters. It is interesting to note that $\rho_0 c_0 = 2.49$ for gold and $\rho_0 c_0 = 2.48$ for silver and Fig. 3 can be approximately used for both metallic NPs simultaneously. The characteristic time τ_0 is approximately equal: $\tau_0 \sim 2 \cdot 10^{-11} - 3.5 \cdot 10^{-9}$ s for the range of radii $r_0 = 10-50$ nm and for ambient water with $k_m = 6 \cdot 10^{-3}$ W/(cmK). Experimental data⁴⁴ confirm a quadratic (parabolic) dependence of characteristic time for energy dissipation versus NP radius $\tau_0 \sim r_0^2$.

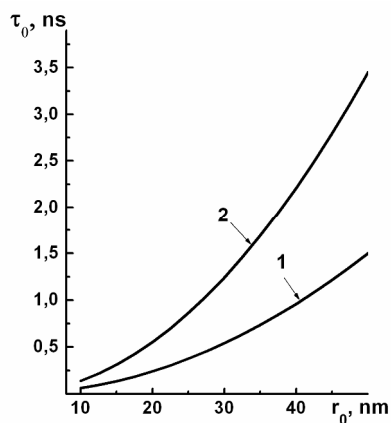


Fig. 4. Dependences of characteristic times of τ_0 (solid lines) on r_0 for gold NPs and ambient water (1) and silica (2).

Figure 5 presents computer and analytical temporal-spatial distributions of the temperature $T(r)$ inside and around NP (left column) for the different time instants t/t_P and temporal distributions of the temperature $T_{max}(r=0, t)$ spherical gold NP with $r_0 = 25$ nm, placed in water, for intensive pulsed irradiation with the pulse durations $t_P = 10^{-8}, 10^{-10}, 10^{-12}$ s. For outer pressure of about $p \sim 100-130$ atm water boiling temperature is approximately equal $\sim 580-603$ K.⁴⁵ For investigation in more wide interval of temperature of NPs, placed in water, we used condition of high outer pressure $p \sim 130$ atm, that allows to heat NP up to $T_0 \sim 580-600$ K as it was used in experiments.³ The temporal-spatial distributions of the temperature $T(r)$ and temporal dependences of the temperature $T_{max}(r=0, t)$ in this case are qualitatively close to the dependences presented in Fig. 2, but they very differ between the maximal values of T_{max} . These results can be applied for the description of experiments with high outer pressure.

Moreover, it should be noted that for short pulses with $t_P = 10^{-8} - 10^{-12}$ s threshold of water explosive evaporation (boiling) is approximately equal $570-590$ K⁴⁶ because of shortening of laser pulse action and these results (Fig. 4) can be used also for external pressure $p \sim 1$ atm.

Figure 6 presents the temporal dependences of $T_{max}(r=0, t)$ on t/t_P for Ag NP with radius $r_0 = 25$ nm placed in silica under the action of short laser pulses. We use intensive fluence (exposure) to achieve melting during NP heating and solidification during cooling of silver NP. The goal of this section is to show the possibility to use analytical dependencies for the description of $T_0(t)$ taking into account possible melting and evaporation of NP.

The processes of melting during the heating under laser pulse action and the solidification during cooling of NP after the termination of radiation action at and upper melting temperature of NP metal (material). The equation taking into account the NP melting has the form

$$\rho_i [c_i + L_M \delta(T - T_M)] \frac{\partial T}{\partial t} = \frac{1}{r^2} \frac{\partial}{\partial r} \left(r^2 k_i \frac{\partial T}{\partial r} \right) + q_i, \quad (23)$$

where T_M is melting temperature, L_M – latent heat of melting, $\delta(x)$ – Dirac delta function, other notations had been mentioned above. The interval of time Δt_M that should be spent for melting of NP under radiation action can be got from energy conservation equation (17), when absorbed radiation energy should be spent for melting and heat exchange with ambience during Δt_M :

$$\Delta t_M \left(\frac{1}{4} I_0 K_{abs} S_0 - J_C S_0 \right) = \rho_0 V_0 L_M,$$

$$\Delta t_M = \frac{4 \rho_0 r_0 L_M}{3(I_0 K_{abs} - 4 J_C)}$$

The interval of time Δt_S that should be spent for solidification of NP during cooling after termination of radiation action can be got from energy conservation equation (17), when energy releasing because of solidification should be spent for heat exchange with ambience

$$\Delta t_S J_C S_0 = \rho_0 V_0 L_M, \quad \Delta t_S = \frac{\rho_0 r_0 L_M}{3 J_C}$$

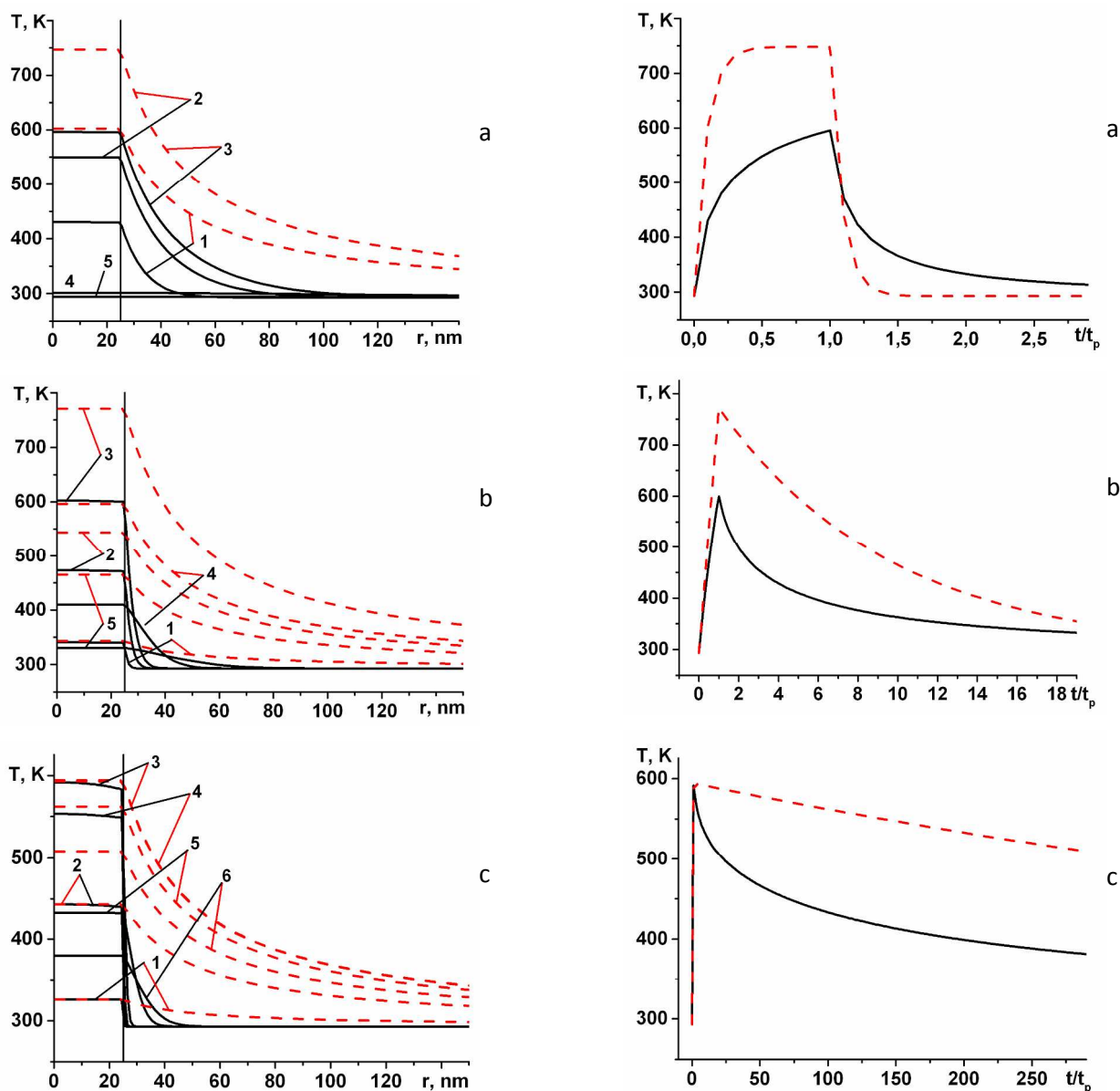


Fig. 5. Computer (solid) and analytical (dashed) dependences of the temperature T along the radius r for the time instants t/t_p (left column) and temporal dependences of $T_{\max}(r=0)$ on t/t_p (right column) for Au NP with $r_0=25$ nm, placed in water: for pulsed irradiation for $t_p=10^{-8}$ s, $l_0=4.3$ MW/cm², $t/t_p=0.1$ (1), 0.5 (2), 1.0 (3), 5.0 (4), 20.0 (5) (a); $t_p=10^{-10}$ s, $l_0=42$ MW/cm², $t/t_p=0.1$ (1), 0.5 (2), 1.0 (3), 5.0 (4), 100 (5) 300 (6) (b); for $t_p=10^{-12}$ s, $l_0=2.5$ GW/cm², $t/t_p=0.1$ (1), 0.5 (2), 1.0 (3), 5.0 (4), 100.0 (5) 300.0 (6) (c). Vertical lines in left column present the boundaries of NP.

The change of NP temperature in time for $t_p = 10^{-8}$ s is shown on Fig. 6a. In this variant duration of a laser pulse t_p is comparable with characteristic time of heat exchange with environment τ_0 . Influence of a pulse of radiation leads to NP temperature increase in time. In analytical model the temperature grows faster, than in numerical model. The melting temperature in analytical calculation is reached earlier, and melting process occurs in the interval of time $\sim 0.05 t_p$, whereas in numerical calculation the interval $\sim 0.13 t_p$. It is connected with formation of the temperature gradient on the characteristic size r_0 in analytical

20

model and in numerical calculation this size appears smaller. As consequence, the thermal flux from a NP surface to environment in numerical calculation appears higher, than in analytical model. After the melting the temperature continues to grow, reaches maximum $T_{\max} = 1945$ K at the moment of $t \sim 0.2 t_p$ and further practically does not vary before the pulse termination (in analytical calculation). After moment $t \sim 0.2 t_p$ the solution follows a quasi-stationary regime when all radiation energy is absorbed by NP and then it is transferred to environment. The temperature grows in numerical calculation up to the termination of laser pulse action and its maximum is equal $T_{\max} = 1670$ K.

Upon termination of a pulse the NP temperature quickly falls and solidification process takes place during the interval of time $0.01 t_p$. We will notice that NP cooling in analytical model occurs faster, than in numerical calculation.

Duration of pulse $t_p=10^{-10}$ s less than characteristic time of heat exchange with environment τ_0 , $t_p < \tau_0$ (Fig. 6b). Influence of pulse

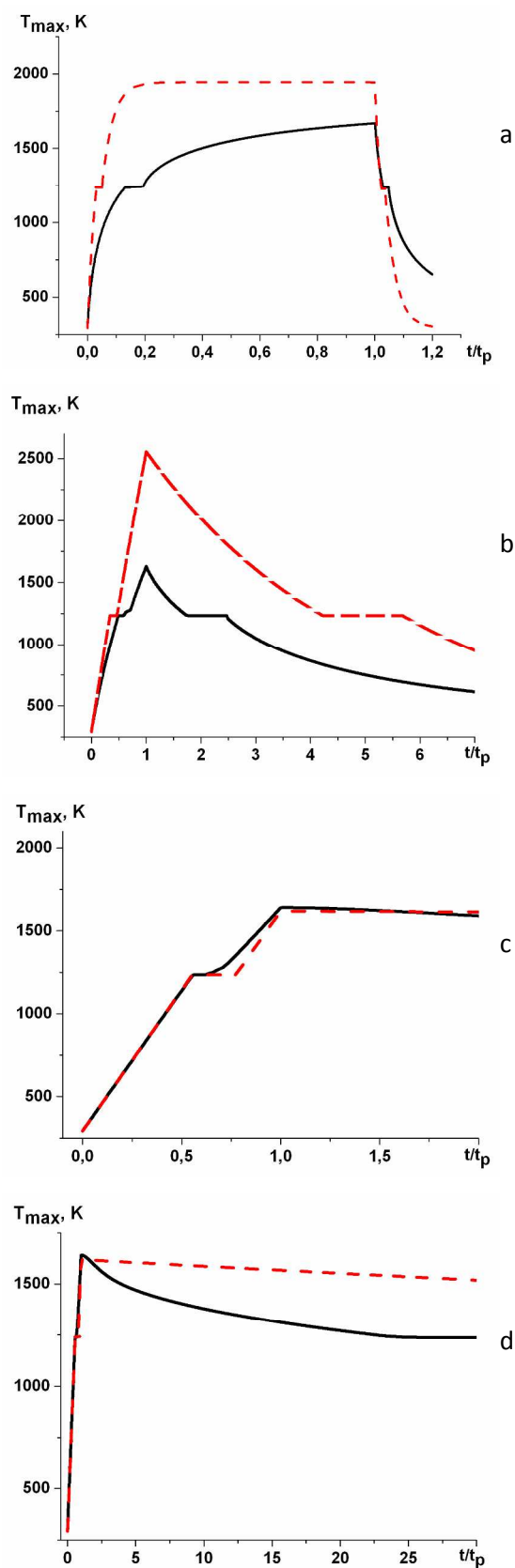


Fig. 6. Computer (solid) and analytical (dashed) temporal dependences of $T_{max}(r=0)$ on t/t_p (right column) for Ag NP with $r_0=25$ nm, placed in silica, for pulsed irradiation with $t_p=10^{-8}$ s, $I_n=37$ MW/cm², (a); $t_p=10^{-10}$ s, $I_n=240$ MW/cm² (b); for $t_p=10^{-12}$ s, $I_n=14$ GW/cm², (c,d).

5 leads to NP temperature increase. The melting temperature in analytical calculation is reached earlier, and melting process occurs in the range of time $0.34 t_p$ whereas in numerical calculation it occurs a bit later - $0.49 t_p$. The temperature continues to grow after the melting, reaches the maximum at the moment of the pulse termination $T_{max} = 2557$ K in analytical model and $T_{max} = 1630$ K - in numerical). Upon termination of an impulse the temperature falls also solidification process take place at interval of time $0.8 t_p$ in analytical model and $1.7 t_p$ - in numerical.

15 The pulse duration $t_p=10^{-12}$ s is much smaller than characteristic time of heat exchange between NP and environment $t_0, t_p \ll \tau_0$ (Fig. 6c). In this case influence of the radiation pulse leads to linear growth of a NP temperature in time practically without heat exchange with ambient silica. The melting temperature in analytical and numerical calculation is reached practically simultaneously at $\sim 0.56 t_p$, and the melting process lasts $\sim 0.1 t_p$ in analytical model and $\sim 0.2 t_p$ - in numerical calculation. The temperature continues to grow after the melting, reaches a maximum at the moment of the pulse termination $T_{max} = 1619$ K in analytical model and $T_{max} = 1640$ K - in numerical.

Conclusion

The problem of optical (laser) radiation heating of NP is important for different applications in laser nanomedicine, laser processing of NPs, light-to-thermal energy conversion and nanoenergy, etc. It is important to theoretically describe the temporal and spatial-temporal behavior of the NP and medium temperature for analysis of experimental results and for theoretical prediction of the unknown dependences and new effects.

35 Unfortunately there is no self-consistent analytical theory^{13,32,37-39} including only real parameters of NP material, environment and laser radiation without using of empirical or adjustable (fitting) parameters that were determined from experiments or used for achievement of some agreement of theoretical dependencies with experimental once.

40 Analytical model has been developed in this article for the description of the thermal processes of heating and melting of single NP under action of CW and pulsed optical (laser) radiation and its cooling and solidification after the termination of radiation action. Presented analytical model demonstrates some advantages in comparison with previous analytical approaches.^{13,32,37-39} Analytical nonlinear expressions for quasi-steady distributions of temperature T and heat flux on radius r around spherical NP and temporal dependences of NP temperature T_0 on t have been conducted and investigated. The temperature dependences of optical and thermo-physical parameters of NPs and surrounding media were taken into account under theoretical modeling of the processes of laser-NP interaction.

45 Dependences of the thermo-optical parameters P_2, P_3 , which characterize the heating efficiency of NPs and the redistribution of absorbed energy between NP and its environment, on the characteristics of NPs and laser radiation were described. The influence of pulse duration on NP heating were investigated in wide interval of pulse durations $t_p \sim 10^{-2}-10^{-12}$ s and for CW irradiation for two cases: 'short' pulses, which allow one to realize the condition of thermal confinement of NPs during laser

pulse action, and ‘long’ pulses, which allow effective heating of the ambient medium. The fulfilment of thermal confinement means achievement of maximal value of NP temperature and saving own heat energy practically without heat exchange with 5 ambience during “short” pulse action with $t_p < \tau_0$. quadratic (parabolic) dependence of characteristic time for energy dissipation versus NP radius $\tau_0 \sim r_0^2$ is confirmed by experimental data.⁴⁴

Developed analytical model for the description of NP heating, 10 heat dissipation and exchange with an ambience has been examined and its accuracy and the regions of its applicability have been estimated and established based on the comparisons and the analysis of the computer and analytical results of the processes of radiation interaction with NP. These comparisons 15 and definite coincidences of the analytical results with the computer results of heating of NPs by CW radiation and laser pulses validate developed analytical model. Computer simulation confirms the possibility to use analytical model for the description of the temporal dependence of NP temperature T_0 for 20 $t_p \geq 10^{-7}$ s, for $10^{-12} < t_p \leq 1 \cdot 10^{-11}$ s and for CW irradiation and outward distributions $T(r)$ for $t_p \geq 10^{-7}$ sand for CW irradiation.

Comparison with results of numerical modeling shows that the presented analytical model gives quantitatively (in determined regions) and qualitatively correct description of dynamics of 25 heating and NP cooling, taking into account its melting and solidification, and the analytical model is quite suitable for the modeling of the thermal processes of the radiation-NP interaction.

References

1. H. Muto, K. Miyajima, F. Mafune, *J. Phys. Chem., B*, 2008, **112**, 5810.
2. Pyatenko, M. Yamaguchi, M. Suzuki, *J. Phys. Chem., B*, 2009, **113**, 9078.
3. S. Hashimoto, D. Werner, T. Uwada, *J. Photochem. Photobiol., C*, 2012, **13**, 28.
4. J. Wang, Y. Chen, X. Chen, J. Hao, M. Yan and M. Qiu, *Optics Express*, 2011, **19**, 14726.
5. Urban, Sol Carretero-Palacios, A. Lutich, T. Lohmüller, J. Feldmann and F. Jäckel, *Nanoscale*, 2014, **6**, 4458.
6. M. Honda, Y. Saito, N. I. Smith, K. Fujita and S. Kawata, *Optics Express*, 2011, **19**, 12375.
7. S. Inasawa, M. Sugiyama, S. Noda and Y. Yamaguchi, *J. Phys. Chem.*, 2006.
8. J-Y. Natoli, L. Gallais, B. Bertussi, A. During, M. Commandre, *Opt. Express*, 2003, **11**, 824.
9. A. Stalmashonak, G. Seifert and A. Abdolvand, Ultra-Short Pulsed Laser Engineered Metal-Glass Nanocomposites. Springer, 2013, 70 p.
10. O. Govorov, H. H. Richardson, *Nano Today*, 2007, **2**, 30.
11. D. Erickson, D. Sinton, D. Psaltis, *Nat. Photon.*, 2011, **5**, 8.
12. V. Pustovalov, L. Astafyeva, W. Fritzsche, *Nano Energy*, 2013, v. **2**, 1137.
13. G. Baffou, H. Rigneault, *Phys. Rev. B*, 2011, **84**, 035415.
14. X. Huang, P. K. Jain, I. H. El-Sayed, M. A. El-Sayed, *Lasers Med. Sci.*, 2008, **23**, 217.
15. L. Kennedy, L. Bickford, N. Lewinsky, et al, *Small*, 2010, **7**, 169.
16. M. A. Philips, M. L. Gran and N. A. Peppas, *Nano Today*, 2010, **5**, 143.
17. V. K. Pustovalov, A. S. Smetannikov and V. P. Zharov, *Laser Phys. Lett.*, 2008, **5**, 775.
18. L. Jianhua, J. Han, Z. Kang, R. Golamally, N. Xu, H. Li and X. Han, *Nanoscale*, 2014, **6**, 5770.

19. R. Narayanan, M. A. El-Sayed, *Top. Catal.*, 2008, **47**, 15.
20. J. R. Adleman, D. A. Boyd, D. G. Goodwin and D. Psaltis, *Nano Lett.*, 2009, **9**, 4417.
21. F. Bohren, D. R. Huffman, Absorption and Scattering of Light by Small Particles. Wiley, New York, 1983.
22. U. Kreibig, M. Vollmer, Optical Properties of Metal Clusters. Springer Series in Material Science Vol 25. Springer, Heidelberg, 1995.
23. Y. Sonnefraud, A. Koh, D. McComb, S. Maier, *Laser Photonics Rev.*, 2012, **6**, 277.
24. V. K. Pustovalov, V. A. Babenko, *Laser Phys. Lett.*, 2004, **1**, 516.
25. P. Jain, X. Huang, I. El-Sayed, M. El-Sayed, *Plasmonics*, 2007, **2**, 107.
26. V. K. Pustovalov, L. Astafyeva, W. Fritzsche, *Science Adv. Mater.*, 2012, **4**, 480.
27. Chen, P. Holt-Hindle, *Chem. Rev.*, 2010, **110**, 3767.
28. S. Yang, X. Luo, *Nanoscale*, 2014, **6**, 4438.
29. M. Rysenga, Cobley, J. Zeng, W. Li, *Chem. Rev.*, 2011, **111**, 3669.
30. Volkov, C. Sevilla and L. Zhigilei, *Appl. Surf. Sci.*, 2007, **253**, 6394.
31. F. Bonneau, P. Combis, J. Ruller et al, *Appl. Phys., B*, 2004, **78**, 447.
32. R. Letfullin, T. George, G. Duree and B. Bollinger, *Adv. Opt. Techn.*, 2008, 251818 (8 pages).
33. E. Sassaroli, K. Li and B. Neill, *Phys. Med. Biol.*, 2009, **54**, 5541.
34. G. Baffou, R. Quidant, F. J. Garcia de Abajo, *ACS Nano*, 2010, **4**, 709.
35. V. Pustovalov, *Laser Phys.*, 2011, **21**, 906.
36. V. K. Pustovalov, *Chem. Phys.*, 2005, **308**, 103.
37. Roper, W. Ahn and M. Hoepfner, *J. Phys. Chem., C*, 2007, **111**, 3636.
38. O. Wilson, X. Hu, D. Cahill and P. Braun, *Phys. Rev., B*, 2002, **66**, 224301.
39. P. Keblinski, D. Cahill, A. Bodapati et al, *J. Appl. Phys.*, 2006, **100**, 054305.
40. V. K. Pustovalov, L. G. Astafyeva, *Laser Phys.*, 2013, **23**, 065.
41. P. B. Johnson, R. W. Christy, *Phys. Rev., B*, 1972, **6**, 4370.
42. Refractive index database, <http://refractiveindex.info/>
43. F. Kreith, W. Z. Black, Basic heat transfer. Harper and Row, New York, 1980.
44. M. Hu, G. Hartland, *J. Phys. Chem. B*, 2002, **106**, 7029
45. Physical Quantities. Eds. I. S. Grigor'ev, E. Z. Meilikhov. Moscow, Atomizdat, 1991 (in Russian).
46. V. P. Skripov, Metastable Liquid. Moscow, Nauka, 1972 (in Russian).

^a Belarusian National Technical University, 220013, Independence pr. 65, Minsk, Belarus, E-mail: pustovalov@mail.ru

^b A.V. Luikov Heat and Mass Transfer Institute of the National Academy of Sciences of Belarus, 220072, P. Brovka str. 15, Minsk, Belarus, e-mail: ass@hmti.ac.by

† Electronic Supplementary Information (ESI) available: [details of any supplementary information available should be included here]. See DOI: 10.1039/b000000x/